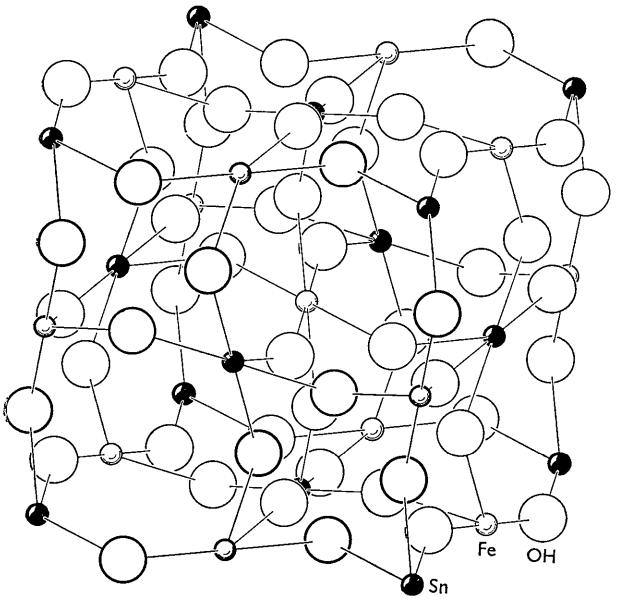

Fig. 3. Die Kristallstruktur von $Fe[Sn(OH)_6]$.

Zur Erklärung der fast erfüllten Reflexbedingungen für ein flächenzentriertes Gitter, ist der Schluss berechtigt, dass die stark streuenden Metallionen 4 Sn^{+4} und 4 Fe^{+2} in der, in O_h^4–$Pn3m$ möglichen flächenzentrierten Verteilung

(*b*) 0, 0, 0; 0, $\frac{1}{2}$, $\frac{1}{2}$; $\frac{1}{2}$, 0, $\frac{1}{2}$; $\frac{1}{2}$, $\frac{1}{2}$, 0

und

(*c*) $\frac{1}{2}$, $\frac{1}{2}$, $\frac{1}{2}$; $\frac{1}{2}$, 0 ,0; 0, $\frac{1}{2}$, 0; 0, 0, $\frac{1}{2}$

vorliegen, während die schwächer streuenden 24$(OH)^-$-Ionen sich in (*k*) *x*, *x*, *z* etc. mit starker Annäherung an flächenzentrierte Verteilung befinden. Durch Vergleich der Reflexabfolge und Intensitäten mit denjenigen von $Fe[Ge(OH)_6]$ (Fig. 1), wovon die Strukturbestimmung mit grosser Verfeinerung vorliegt (Strunz & Giglio, 1959), wird *x*, *x*, *z* nur wenig von 0, 0, $\frac{1}{4}$ verschieden sein. Durch Vergleich der beobachteten Gitterdimensionen mit den additiv aus den bekannten Ionenradien gefundenen Werten ist für

$$Fe[Sn(OH)_6]: x=0{,}056, \quad z=0{,}248 .$$

Damit berechnen sich die in Fig. 2 angeführten Intensitäten, deren Übereinstimmung mit der experimentellen Beobachtung gut ist. Sn und Fe sind pesudooktaedrisch von 6 (OH) umgeben; die genannten Stannate sind isotyp, streng genommen homöotyp, mit $Fe[Ge(OH)_6]$ und den von Schrewelius (1938) untersuchten Verbindungen $NaSb(OH)_6$ und $AgSb(OH)_6$. Die Formeln $MnSnO_3.3\,H_2O$, $CoSnO_3.2\,H_2O$ etc. (Coffeen, 1953) konnten nicht bestätigt werden.

Bei der technischen Auswertung der Röntgenaufnahmen hatten wir dankenswerterweise die Hilfe von Herrn W. Stahn.

Literatur

COFFEEN, S. W. (1953). *J. Amer. Ceram. Soc.* **36**, 207.
SCHREWELIUS, N. (1938). *Z. anorg. Chem.* **238**, 241.
STRUNZ, H., SÖHNGE, G. & GEIER, B. H. (1958). *Neues Jb. Miner., Mh.* p. 85.
STRUNZ, H. & GIGLIO, M. (1959). *Naturwiss.* **46**, 489.

Acta Cryst. (1960). **13**, 603

Stacking Faults in Iron-Manganese and Cobalt-Nickel

BY J. SPREADBOROUGH*

Department of Metallurgy, University Museum, Oxford, England

(*Received* 20 *July* 1959 *and in revised form* 15 *December* 1959)

The results of applying the methods which may be used to measure the fault parameters in hexagonal and cubic materials are presented and discussed for a cobalt–nickel alloy. Studies of iron–manganese alloys show that the epsilon phase faults readily; this factor may contribute to the high work-hardening capacity of such alloys.

1. Introduction

Stacking faults have been measured by X-ray methods in both close-packed metallic structures (Warren & Warekois, 1955; Anantharaman & Christian, 1956; Christian & Spreadborough, 1956, 1957; Smallman & Westmacott, 1957). The work reported here is concerned with faults in a Co–Ni hexagonal alloy and in the ε-phase in Fe–Mn.

The Co–Ni hexagonal alloy was chosen partly because it was thought likely to contain heavy faulting after deformation and partly because the application of the methods used previously to estimate faulting in hexagonal materials (Fourier analysis and line-breadth measurements) would be interesting for high

* Now at Battelle Memorial Institute, Geneva, Switzerland.

values of faulting, and might provide a comparison of the relative reliability and usefulness of the methods in such cases.

The iron–manganese and iron–manganese–carbon alloys are of interest, owing to their large work-hardening capacities; these have been attributed to the formation of the metastable ε-phase (close-packed hexagonal). The present experiments were made to see if stacking faults occurred in this phase as they might be responsible, in part at least, for the work-hardening capacity of alloys containing ε.

2. Hexagonal cobalt-nickel

An alloy containing ~78 wt.% cobalt was used; it was taken from the ingot KOP. I. used by Taylor (1950) for measurements of the lattice spacing of cobalt–nickel alloys.

After homogenizing at 1100 °C. in vacuo, filings were taken, made into a diffractometer specimen and examined in the Norelco instrument, using Co $K\alpha$ X-rays. Only three weak lines were visible on the chart record, corresponding to the $10\bar{1}0$, 0002 and $10\bar{1}1$ hexagonal lines, whose tails overlapped considerably. On detailed examination a hump corresponding to the 200 cubic line was found. The full range of these lines was scanned by hand at small intervals of 2θ with a minimum count of 1600 at each point in a continuous sequence. A form of Rachinger's graphical method was used to resolve the lines first, and then their respective α_1 components (Rachinger, 1948).

The α_1 profiles of the $10\bar{1}1$ and 0002 lines were taken for Fourier analysis, using the 0002 as standard. The method used by Anantharaman & Christian (1956) was followed. From the linear portion of the graph of A_n versus n, α was calculated to be 0·145 or ~1 plane in 7 faulted. This is by far the largest fault value found so far for metals. No lines of even L index were visible and so a direct demonstration that only deformation faults were present was not possible; however, Anantharaman & Christian showed that for a deformed cobalt specimen deformation faults predominated.

The specimen was then annealed for 3 hr. at 250°, just below the transformation temperature for an alloy of this composition (Barrett & Hess, 1952), and the profiles remeasured. Annealing the specimen for three hr. at 800 °C. and slow cooling retained the cubic phase completely. Quenching in liquid air did not effect any transformation, and so the specimen was given a long heat treatment to increase particle size and favour transformation. Subsequent examination showed no trace of hexagonal, but a liquid-air quench produced weak hexagonal reflections, corresponding to the $10\bar{1}0$, $10\bar{1}1$, $11\bar{2}0$ and $11\bar{2}2$ lines, as well as the strong cubic lines. Fourier analysis of the $10\bar{1}1$ shape using the 200 cubic as standard gave a good linear plot for $A_n - n$. The cubic 200 was measured carefully before and after quenching. The α_1 peak shifted slightly, suggesting that deformation faults were introduced in the cubic by the quenching strains. A Fourier analysis was made of the 200 after quench using the before quenched 200 profile as standard.

Line breadth measurements were made on all the lines treated by Fourier analysis, and α calculated from them, after making the usual corrections for limitation of measuring range, etc.

A comparison of the results obtained by the two methods is given in Table 1, which also includes the results for cubic deformation faulting. Although the 200 was faint in the original deformed specimen, a noticeable shift occurred after annealing at 800 °C., which corresponded to a high value of α for cubic deformation faulting. The amount of hexagonal phase present was estimated from the integrated intensities of the $10\bar{1}0$ and 200 lines, after correction for changes in intensity due to faults and insufficient measuring range.

The agreement between the Fourier and line-breadth results for the deformed specimen is extremely poor.

Table 1. *Summary of results for* Co–Ni (78–22)

Treatment	Estimated % hexagonal	Type of fault and α: Hex. growth	Hex. defn.	Cubic defn.	Method used
Cold worked filings from ingot	>90%	Assumed	0·145	—	F. ($10\bar{1}1$), (0002) standard
		nil	0·075	—	L.B. ($10\bar{1}1$), (0002) standard
		—	—	~0·03	P.S. (200) on annealing to cubic
Annealed 3 hr. at 250 °C.	>90%	Assumed	0·116	—	F. } as above
		nil	0·045	—	L.B. } as above
		—	—	~0·03	P.S. } as above
Long heat treatment and slow cool from 1,000 °C., followed by liquid air quench	~10%	0·109	—	—	F. ($10\bar{1}1$), (200) before quench as standard
		0·111	—	—	F. ($10\bar{1}1$), (200) after quench as standard
		0·114	—	—	L.B. ($10\bar{1}1$), (200) before quench
		0·107	—	—	L.B. ($10\bar{1}1$), (200) after quench
		—	—	0·003	P.S. (200) before and after quenching
		—	—	0·004	L.B. as above
		—	—	0·003	F. as above
		—	—	0·003	L.B. (220) after quench ($11\bar{2}0$) as standard

F. = Fourier Analysis Method. L.B. = Line Breadth Method. P.S. = Peak Shift Method.

The determination of the line profiles of such broad weak lines is difficult and it is likely that the background levels were in error by a few per cent of the peak intensity. Anantharaman & Christian (1956) carried out a numerical analysis on a theoretical line shape assuming a value for α in the case of hexagonal growth faults. They calculated the true intensity values and also those obtained if the background level were taken too high with respect to the peak. The calculated A_n values corresponded to the theoretical ones at $n>4$ and $n>6$ for a background raised by 1% and 2% respectively of the peak intensity. Similar calculations for the case of hexagonal deformation faults have been made by the author. The effect of tail errors is to curve the initial part of the graph of $\log A_n$ against n, as found in practice in the present work.

For the cold-worked specimen, the lines were considerably broadened by strain. Thus the error in the determination of the integral breadth was probably large compared to the errors in the line shape. The Fourier method is not so sensitive to the location of the background level or the tail errors, since the *shape* of the more intense part of the line profile is more important. It should also be noted that the diffraction line used was the $10\bar{1}1$; for such a line of odd L index the theoretical broadening for $\alpha=0{\cdot}1$ in the case of deformation faults is approximately three times that for growth faults. Thus any discrepancies between the Fourier and line-breadth results would be expected to be more pronounced for a deformation-faulted specimen than for one containing growth faults.

The agreement between the Fourier and line-breadth results is good for the growth-faulted specimen, where the measurement of line breadth was easier. Thus it may be tentatively concluded that either method may be used for studies of heavy growth faulting (the values reported here seem to be the highest so far found), but that in dealing with broad weak lines, such as those from a specimen containing heavy deformation faulting, the Fourier method is more reliable.

All three methods for determining the cubic deformation faulting introduced by quenching give the same value.

The results of using the before-quenched or after-quenched profiles of the (200) as standards for calculating the hexagonal growth faulting are identical to within the experimental error for both the line-breadth and Fourier results.

3. Iron-manganese

Alloys of pure iron and pure manganese were available from work in this laboratory on the Fe–Mn phase diagram (Hellawell & Hume-Rothery, 1957). Ingots were annealed in argon at 1100 °C. for three hr. and quenched into ice-water. Filings were taken from the ingots and examined in a Norelco diffractometer with Fe $K\alpha$ radiation. Filings were also annealed at 1100 °C. in argon for $\frac{1}{2}$ hr. in silica capsules and the capsules dropped into crushed ice. For the 8·6 at.% and 11·9 at.% Mn alloy, both the cold worked and annealed filings showed only b.c.c. (ferrite) lines.

The annealed filings of the 13·8 at.% Mn alloy contained a small amount ($<10\%$) of hexagonal ε-phase. Careful hand scans were made of the region 50–64° 2θ, containing the $10\bar{1}0$, 0002 and $10\bar{1}1$ hexagonal lines and the 110 b.c.c. line. The 0002 line was too near the 110 b.c.c. for use as standard in determining the line breadth, so the $10\bar{1}0$ was used as standard for the $10\bar{1}1$. From the breadth due to faulting the parameter α was found to be 0·025 for growth faults, i.e. ~ 1 plane in 40. As no hexagonal lines of type $10\bar{1}2$ were visible it was not possible to decide whether the broadening was due to growth or deformation faulting. (The powder was cold-worked slightly in preparing the specimen.) If the broadening were entirely due to deformation faults α deformation would be $=0{\cdot}015$.

As the amount of ε formed in this system is very sensitive to degree of deformation and particle size, systematic studies of this system are difficult; accordingly the demonstration that the ε-phase is faulted is probably all that can profitably be achieved.

Since the completion of this work, Otte (1957) has published the results of his examinations of solid specimens of Fe–Mn–C (a Hadfield steel); no non-Laue streaks were found on the oscillation X-ray patterns when the sample was deformed at 4 °K., but microphotographs were cited as evidence for faulting in the austenite. Thus some complexity probably exists in deformed Fe–Mn or Fe–Mn–C with both the f.c.c. austenite and c.p.h. ε faulted, analogous to the cobalt–nickel alloy examined during the present work.

The writer wishes to thank Dr J. W. Christian for helpful discussions and Prof. W. Hume-Rothery, F.R.S. for laboratory accommodation and for his encouragement of this work.

References

Anantharaman, T. R. & Christian, J. W. (1956). *Acta Cryst.* **9**, 479.
Barrett, C. S. & Hess, J. B. (1952). *J. Metals*, **4**, 645.
Christian, J. W. & Spreadborough, J. (1956). *Phil. Mag.* **1**, 1069.
Christian, J. W. & Spreadborough, J. (1957). *Proc. Phys. Soc. Lond.* B, **70**, 1151.
Hellawell, A. & Hume-Rothery, W. (1957). *Philos. Trans.* A, **241**, 417.
Otte, H. M. (1957). *Acta Met.* **5**, 614.
Rachinger, W. A. (1948). *J. Sci. Instrum.* **25**, 254.
Smallman, R. E. & Westmacott, K. H. (1957). *Phil. Mag.* **2**, 669.
Taylor, A. (1950). *J. Inst. Met.* **77**, 585.
Warren, B. E. & Warekois, E. P. (1955). *Acta Met.* **3**, 473.